Calculated polarizabilities of intermediate-size Si clusters

Koblar Jackson
Department of Physics, Central Michigan University, Mount Pleasant, Michigan 48859

Mark Pederson
Complex Systems Theory Branch, U.S. Naval Research Laboratory, Washington D.C. 20375

Cai-Zhuang Wang and Kai-Ming Ho
Ames Laboratory, U.S. Department of Energy and Department of Physics and Astronomy, Iowa State University, Ames, Iowa 50011
(Received 5 January 1999)

We have used a first-principles, density-functional-based method to calculate the electric polarizabilities and dipole moments for several low-energy geometries of Si clusters in the size range $10 \leqslant N \leqslant 20$. The polarizability per atom is found to be a slowly varying, nonmonotonic function of N. Over this size range the polarizability appears to be correlated most strongly to cluster shape and not with either the dipole moment or the highest occupied–lowest unoccupied molecular-orbital gap. The calculations indicate that the polarizability per atom for Si clusters approaches the bulk limit from above as a function of size. [S1050-2947(99)07305-9]

PACS number(s): 36.40.−c, 36.40.Cg, 61.46.+w, 71.24.+q

I. INTRODUCTION

One of the fundamental goals of cluster science is to understand how the properties of clusters evolve with cluster size. Progress toward this goal has been slow, however, due in part to a lack of reliable information about the arrangement of the atoms in clusters. Recently, some of us used an accurate tight-binding model combined with a powerful genetic algorithm (GA)-based search technique to identify the likely equilibrium structures for Si clusters in the size range $10 \leqslant N \leqslant 20$ [1]. The structures were further optimized using first-principles, local-density approximation (LDA) [2,3] calculations, and were checked for consistency with experimental, ion mobility data [1]. Further analysis of the ionization potentials of these clusters [4] and of the cluster dissociation energies [5] (and hence binding energies) firmly establishes these structures as the species observed in the experiments.

Combining the new structures with those for $N \leqslant 10$ that were previously known, it is now possible to shift attention to the physical properties of the Si clusters, to study how they behave over the $1 \leqslant N \leqslant 20$ atom size range. In this paper we focus on the electric polarizabilities of the clusters. The polarizability is a basic property of an electronic system, related in the bulk limit to the static dielectric constant. It is of particular interest for Si clusters because it can be seen as a rough measure of the ''metallic'' character of the clusters as compared with the semiconducting nature of bulk Si. It is also possible that comparisons between measured and computed polarizabilities may be used to help identify cluster structures [6].

Electric polarizabilities for small Si clusters in the range $1 \leqslant N \leqslant 10$ have been computed previously using first-principles methods [7–9], as well as values for selected other Si cluster models [10]. The basic result of these calculations is that the polarizability per atom of the small clusters is larger than the corresponding value for bulk Si, inferred from the bulk dielectric constant on the basis of the Clausius-Mossotti relation. This has been interpreted in terms of the enhanced polarizability of electrons in dangling-bond states on the cluster surfaces [7]. Here we show that this trend continues for clusters in the range $10 \leqslant N \leqslant 20$.

In Sec. II we discuss our LDA-based method for computing cluster polarizabilities. We then present and discuss the results of the calculations. We end the paper with a brief summary.

II. COMPUTATIONAL METHOD

To determine the cluster polarizabilities using the LDA, an external electric field **F** is introduced into the standard LDA calculation. The field adds a term to the potential ''seen'' by the electrons:

$$V_{\mathrm{ext}} = -e\mathbf{r}\cdot\mathbf{F}. \tag{1}$$

The Kohn-Sham equations are solved self-consistently in the presence of this extra potential, and the resulting orbital wave functions are used to evaluate the total energy in the presence of the external field. The mean cluster polarizability is then defined as

$$\bar{\alpha} = \frac{1}{3}\mathrm{Tr}[\boldsymbol{\alpha}], \tag{2}$$

where the elements of the polarizability tensor are

$$\alpha_{ij} = -\frac{\partial^2 E}{\partial F_i \partial F_j} = \frac{\partial \mu_i}{\partial F_j}. \tag{3}$$

Here E is the cluster total energy and μ_i is a component of the cluster electric dipole. The polarizability is evaluated using a finite difference approach, in which

$$\alpha_{ii} = \frac{\mu_i(\delta F_i) - \mu_i(-\delta F_i)}{2\,\delta F_i}. \tag{4}$$

 ©1999 The American Physical Society

TABLE I. Calculated binding energies E_b, HOMO-LUMO gaps E_g, dipole moments (μ), and polarizabilities (α) for Si_n. The values listed for the clusters through Si_{10} are taken from Ref. [8]. The values for Si_{20c} and Si_{21} are taken from Refs. [15] and [10]. The values for E_b include a small, systematic shift of about 0.02 eV/atom when compared to the results in Ref. [4] The differences are due to the use of different LDA functionals.

Cluster	E_b/atom (eV)	E_g (eV)	μ (Debye)	α (Å^3)
Si_1	-	-	0.00	5.88
Si_2	−1.994	0.00	0.00	7.84
Si_3	−2.965	1.01	0.32	5.21
Si_4	−3.541	1.07	0.00	5.07
Si_5	−3.825	1.98	0.01	4.82
Si_6	−4.041	2.11	0.21	4.51
Si_7	−4.187	2.10	0.00	4.36
Si_8	−4.122	1.42	0.00	4.54
Si_9	−4.234	1.99	0.28	4.38
Si_{10}	−4.357	2.03	0.73	4.32
Si_{11}	−4.292	1.06	0.82	4.51
Si_{12}	−4.324	2.12	0.14	4.59
Si_{13}	−4.322	0.93	1.22	4.52
Si_{14}	−4.368	1.70	1.06	4.52
Si_{15}	−4.397	2.11	2.32	4.55
Si_{16a}	−4.352	0.64	0.00	4.79
Si_{16b}	−4.350	1.64	0.00	4.66
Si_{17}	−4.400	1.49	1.01	4.80
Si_{18a}	−4.418	1.90	3.98	4.88
Si_{18b}	−4.405	0.57	0.00	4.80
Si_{19a}	−4.426	0.87	1.08	4.58
Si_{19b}	−4.411	1.15	3.32	4.88
Si_{20a}	−4.432	0.97	1.04	4.55
Si_{20b}	−4.417	0.79	0.18	5.22
Si_{20c}	−4.37	0.84	0.02	4.83
Si_{21}	−4.40	0.54	0.79	4.58

We use a field strength of $\delta F_i = 0.005$ a.u. to evaluate the derivatives. Fields of this size have been shown to yield well-converged results for the derivative [7,11].

The field strength used in the calculations corresponds to about 2.6×10^9 V/m, or about two orders of magnitude larger than typical laboratory fields used to make polarizability measurements [6] (about 2×10^7 V/m). For the calculated dipole moments and polarizabilities for Si clusters discussed below, the energy shifts of the clusters in the laboratory field would be very small. For the largest dipole moment calculated (3.98 D for Si_{18a}; see Table I), the energy gained by aligning the dipole in the laboratory field would be only about 1.6×10^{-3} eV. This is over an order of magnitude smaller than kT at room temperature, and two orders of magnitude smaller than typical total energy differences between cluster isomers (e.g., 0.27 eV for the two lowest energy Si_{18} isomers) [12]. The laboratory fields are thus not large enough to affect the energy balance between competing low-energy structures.

The calculations reported here were performed using an all-electron, Gaussian-orbital-based implementation of the LDA known as NRLMOL [13,14]. The NRLMOL codes feature an accurate numerical integration scheme for evaluating cluster total energies and electric dipoles. We use large basis sets including six *s*-type, five *p*-type, and four *d*-type orbitals centered on each atom, to insure convergence of the results with respect to basis sets [15]. We use the exchange-correlation functional of Perdew, Burke, and Ernzerhof [16] (PBE), at the LDA level. Benchmark calculations on small hydrocarbons and the water molecule found that gradient corrections to the LDA had only a minor impact on calculated polarizabilities [11]. To test this directly for Si clusters, we computed the polarizability of Si_{11} at both the LDA and generalized gradient approximation (GGA) levels of theory, obtaining 4.51 and 4.53 Å^3, respectively. Because of the small differences between LDA and GGA values, we opt to use the simpler LDA level of theory here.

For the clusters in the range $11\leqslant N\leqslant 20$, we used the new structures obtained by Ho *et al.* [1], without additional relaxation. Since these structures were not obtained using the NRLMOL codes, we first explicitly tested the structures to insure that numerical differences between independent LDA codes would not lead to significant differences in optimized structures. We reoptimized the structure for Si_{12} within the NRLMOL codes, starting from the Ho *et al.* geometry. The additional relaxation was very small, changing the total energy of the cluster by only 0.02 eV. The change in the calculated polarizability was also very small, from 4.59 to 4.54 Å^3 for the unrelaxed and relaxed structures, respectively.

III. RESULTS AND DISCUSSION

The basic results of our calculations are tabulated in Table I, where we list the binding energy per atom (E_b), highest occupied–lowest unoccupied molecular-orbital (HOMO-LUMO) gap (E_g), dipole moment (μ), and mean polarizability per atom (α), for the lowest-energy clusters with $11\leqslant N\leqslant 20$. The GA search produced two isomers differing in binding energy by less than 0.02 eV/atom for $N=16$ and 18–20. Results are shown in Table I for each of these structures. We also include previous results [8] for Si_N with $1\leqslant N\leqslant 10$ for completeness, as well as results for two additional isomers, one for Si_{20} (referred to below as Si_{20c}) and one for Si_{21} [15].

A note is in order regarding the value of the polarizability of Si_2. The value shown in Table I, 7.84 Å^3/atom, was obtained for the ground state of the dimer, a spin triplet state with a bond length of 2.270 Å. The paramagnetic state of the dimer lies above the triplet state in energy, and has a shorter bond length of 2.195 Å. The polarizability of the paramagnetic dimer was found to be 6.40 Å^3/atom. This latter value is in good agreement with the value 6.29 Å^3/atom reported earlier [7], and suggests that that calculation was based on the paramagnetic state.

In Fig. 1 we show for reference the proposed equilibrium structure for Si_{10} and the two lowest-energy models for Si_{18} and Si_{20}, respectively. Si_{10}, Si_{18a}, Si_{18b}, and Si_{20b} all contain the basic building block that appears in most of the equilibrium structures over this range, the tricapped trigonal prism (TTP) [1]. In Si_{10}, the TTP unit is seen from the side, with a cap atom added to the top face of the prism; Si_{18a} is a stack of a TTP unit and a distorted TTP unit; Si_{18b} is a symmetric stack of two TTP units; and Si_{20b} is a quasisym-

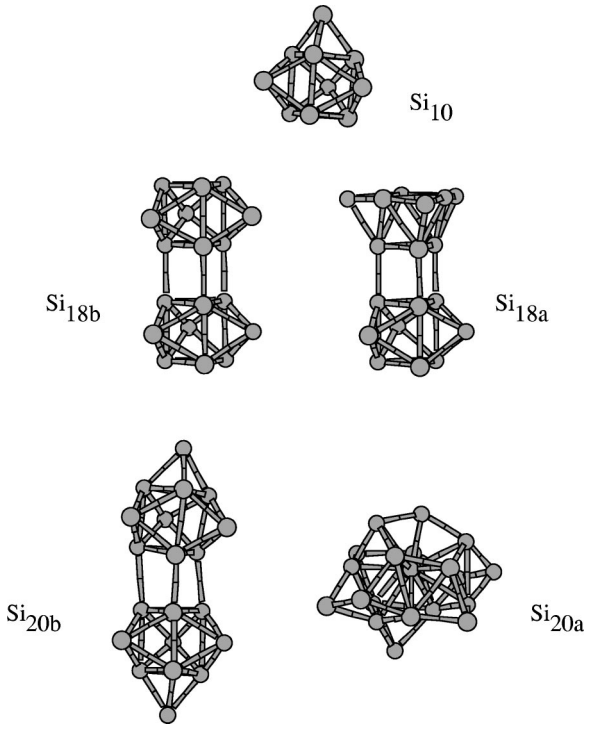

FIG. 1. Cluster structures for selected Si clusters in the $10 \leqslant N \leqslant 20$ size range. Depicted are Si_{10}, two prolate isomers for Si_{18}, and one prolate and one compact isomer for Si_{20}.

metric stack of two Si_{10} units. The compact structure of Si_{20a} is clearly different from the prolate Si_{20b} isomer.

The results in Table I show that among the properties listed only E_b, the cluster binding energy, changes smoothly over this size range. E_g and μ change dramatically from cluster to cluster with no overall trend. The values for α also show significant variation, but with an apparent correlation to overall cluster shape that we now discuss.

If we focus on the range Si_{10}–Si_{20}, the clusters up to Si_{15} have relatively compact structures that can be viewed as TTP units with capping atoms added to various faces and/or edges, as in the case of Si_{10}, depicted in Fig. 1. Beginning with Si_{15}, the structures can be described as a TTP unit with an additional structure bonded to an end face of the prism. This stacking of structures increases the aspect ratio of the clusters, making them increasingly prolate. The stacking trend continues over the larger clusters in the range, culminating in the Si_{20b} structure shown in the figure, a stack of two Si_{10}'s. The polarizabilities of these clusters increase as they become more prolate, from 4.55 Å^3 for Si_{15} to 5.22 Å^3 for Si_{20b}. For the compact isomers Si_{19a} and Si_{20a}, the polarizabilities are considerably smaller, 4.58 and 4.55 Å^3, in line with the values found for the clusters with $N<15$.

These values of the polarizability for prolate and compact clusters are consistent with the values found previously for a compact isomer of Si_{21}, 4.58 Å^3, and for a prolate isomer of Si_{20}, 4.83 Å^3 [10]. The Si_{21} model is roughly similar to the Si_{20a} structure shown in Fig. 1, while the Si_{20c} structure features a significantly different arrangement of the atoms than the prolate isomers for Si_{18}–Si_{20}. The fact that the polarizabiity of these models are similar to those found for the other compact and prolate clusters reinforces the idea that the polarizability can be related to cluster shape, rather than to the detailed arrangements of the atoms.

What accounts for the systematic difference in the polarizability for compact versus prolate clusters? Simple one-electron perturbation theory of the polarizability yields

$$\alpha_{xx}=2\sum_{k,l}{}' \frac{e^2|\langle k|x|l\rangle|^2}{\epsilon_l-\epsilon_k} \tag{5}$$

where the one electron matrix elements are between occupied and unoccupied orbitals, and $\epsilon_l-\epsilon_k$ is the corresponding transition energy. (The prime over the summation indicated that terms with $k=l$ are to be omitted.) Focusing on the energy denominator, this expression suggests the rough rule of thumb that $\bar{\alpha}$ should be inversely proportional to E_g, the cluster HOMO-LUMO gap. However, Vasiliev, Ogut, and Chelikowsky [7] pointed out that contributions from transitions above E_g can dominate this expression, and they showed that the inverse relationship between $\bar{\alpha}$ and E_g does not hold in general.

The values in Table I also show that there is no simple relationship between $\bar{\alpha}$ and E_g for Si clusters in this size range. In some cases a cluster that has a large value of E_g has a large value of $\bar{\alpha}$ as well, while in other cases the opposite is true. An interesting example is provided by the two Si_{18} isomers shown in Fig. 1. Both are prolate, but one is a symmetric stack of nearly ideal TTP units, while the other is a TTP unit plus a very distorted TTP unit. The latter structure has a much larger band gap, 1.90 versus 0.57 eV, but the polarizabilities for the clusters are very similar, 4.88 Å^3 vs 4.80 Å^3. In this example, E_g is seen to be a local property of the cluster, related to a local rearrangement of the atoms, whereas the polarizability is apparently tied to the overall shape of the cluster.

There is also little correlation between cluster dipole moment, μ, and $\bar{\alpha}$ in Table I. The value of μ fluctuates considerably from cluster to cluster, and reflects primarily the cluster symmetry. Components of the electric dipole in directions perpendicular to either reflection planes or rotation axes must vanish by symmetry. Highly symmetric clusters thus have small or vanishing dipole moments. The two prolate Si_{18} isomers again provide a good example. Si_{18b} is a symmetric stack of TTP units, and it thus has a vanishing dipole moment. The symmetry in the stacking direction is broken in Si_{18a}, however, resulting in a different distribution of electron charge density in the upper and lower halves of the structure and a large dipole moment of 3.98 D.

To understand the differences in α between prolate and compact clusters it is useful to consider some of the implications of these shapes on bonding in the clusters. In Table II we show the average coordination numbers and mean bond lengths for the compact and prolate isomers for Si_{19} and Si_{20}. As shown in the table, the prolate structures have higher coordination numbers and longer bond lengths than the compact structures. (Here we have done the bond counting by assuming a bond to exist between any two atoms separated by 2.6 Å or less.) The connection between average coordination number and bond length has a ready physical interpretation. The greater the number of bonds in a cluster, the smaller the valence charge density that can be associated

TABLE II. Average coordination number, $\langle n \rangle$, average bond length $\bar{r}$, and polarizability α for compact (Si_{19a} and Si_{20a}) and prolate (Si_{19b} and Si_{20b}) clusters.

Cluster	$\langle n \rangle$	$\bar{r}$ (Å)	α
Si_{19a}	3.47	2.44	4.58
Si_{19b}	4.21	2.46	4.88
Si_{20a}	3.20	2.40	4.55
Si_{20b}	4.40	2.47	5.21

with each individual bond. Each bond is then weaker, and thus somewhat longer than in a comparable system with fewer bonds. That the individual bonds are weaker in the prolate structures can be seen by comparing the binding energy *per bond* for the different Si_{19} and Si_{20} isomers. For the compact structures we obtain 2.6 eV and 2.8 eV/bond, respectively, but only 2.1 and 2.0 eV/bond for the prolate isomers.

A rationale for the polarizability trends can now be given. The compact structures have relatively fewer and shorter bonds, binding the valence electrons tighter and in a smaller spatial volume than the prolate clusters. Since atomic polarizabilities can be related to the volume occupied by the electrons, we can expect smaller polarizabilities for the compact clusters than for the prolate clusters. The same qualitative result linking the polarizability to the volume occupied by the orbitals can be obtained from perturbation theory [17], although the broad assumptions required in the derivation make it difficult to apply the result in more than a qualitative way.

The atomic arrangements seen in Fig. 1 are clearly very different from the bulk Si diamond structure. It is therefore not surprising that the cluster properties shown in Table I are far from the corresponding bulk values. The LDA value for the bulk cohesive energy, 5.38 eV/atom [18], for example, far exceeds the cluster binding energies given in the table. To obtain a bulk value for the polarizability per atom we can use the Clausius-Mossotti relation

$$\bar{\alpha} = \frac{3}{4\pi}\left(\frac{\epsilon - 1}{\epsilon + 2}\right) v_{\mathrm{at}}, \tag{6}$$

where v_{at} is the volume per Si atom in the Si unit cell, and ϵ is the static dielectric constant of the bulk. Taking $\epsilon = 11.8$ and $v_{\mathrm{at}} = 19.47$ (the latter also from the LDA calculation of Ref. [18]) we arrive at a value for the bulk atomic polarizability of 3.64 $Å^3$/atom. This value is considerably smaller than the values for the clusters in Table I. Note that $\bar{\alpha}$ for the compact isomers is much closer to the bulk value. The fact that the bulk value is so small can be understood on the basis of the argument given above, inasmuch as the short bulk bond lengths (2.33 Å) correspond to smaller effective volumes for the valence electrons and thus a smaller polarizability than in the clusters.

The systematic differences between the values of $\bar{\alpha}$ for prolate and compact clusters are interesting in light of experiments that show that a shape transition from prolate to compact structures occurs for Si clusters at around 26 atoms [19]. According to the results in Table I, we would expect to see a transition in the value of the cluster polarizability from values around 5.0 $Å^3$ to values closer to 4.5 $Å^3$ over this size range. Since the measurements would average over the polarizabilities of all the clusters present, the transition may be gradual, rather than steplike, depending on the relative population of prolate versus compact clusters present over the transition region.

Polarizabilities for Si clusters between nine and 120 atoms have been measured recently [6,20,21]. In contrast to our calculated results, which show relatively small variations in the value of $\bar{\alpha}$ over the size range $10 \leqslant N \leqslant 20$, with all values significantly larger than the bulk limit, the measurements show large variations in $\bar{\alpha}$ over this range and an average value lying significantly below the bulk limit. The experimental data include large error bars, which may explain the differences between theory and experiment. It would be interesting to see measurements that improve on the error bars in Ref. [6]. For example, in order observe a transition in polarizabilities coinciding with a shape transition in the clusters, the measurements would need to resolve changes on the order of 10%. There is no clear transition in the value of $\bar{\alpha}$ occuring at around $N = 26$ in the current data [6]. We note, for reference, that the polarizabilities for alkali and aluminum clusters are known to decrease with size and approach the bulk limit from above [22,23].

A close agreement between theory and experiment would require that temperature effects be taken into account. At low temperatures the dipole moment of a cluster tends to align with an external field. This alignment has the effect of contibuting an extra term to the cluster's polarizability. The total effective polarizability can be shown to be

$$\bar{\alpha}_{\mathrm{eff}} = \bar{\alpha} + \frac{\mu^2}{3kT}. \tag{7}$$

For clusters with large dipole moments like Si_{15}, Si_{18a} and Si_{19b}, the second term is roughly equal to $\bar{\alpha}$ at room temperature. At low temperatures the dipole-related term dominates $\bar{\alpha}$ for these clusters. Since the prolate clusters tend to have larger dipole moments than the compact clusters, accurately measuring cluster dipole moments could be another approach to identifying cluster shape transitions. An important point in this context is that the expression for the effective polarizability given above assumes the clusters to be in thermal equilibrium in the external field. This condition may not be satisfied in beam experiments in which the clusters spend a very short time in the external field.

While experiments [19] have shown the prolate to compact transition to occur at $N = 26$, the E_b results in Table I suggest that the compact structures are already much more stable at $N = 19$. This apparent contradiction may be resolved in part by noting that atomization energies are well known to be overestimated in the LDA, a situation that is corrected to some extent using gradient-corrected functionals (GGA's) [24]. We have found previously that the GGA systematically favors prolate Si clusters over compact ones [25]. To test whether this trend holds for the clusters studied here, we computed the GGA binding energies for Si_{20a} and Si_{20b}, using the relaxed LDA geometries for both. Within the PBE form of the LDA, Si_{20a} is 0.49 eV more stable than Si_{20b}. In

the PBE version of the GGA, the two structures are essentially degenerate, with the compact structures being lower by only 0.02 eV. Thus the GGA results indicate that at $N=20$, the prolate clusters are essentially isoenergetic with the compact structures. These results are in complete agreement with the calculations of Ref. [4], where similar calculations were done using different GGA functionals.

IV. SUMMARY

In this paper we have presented calculated electric polarizabilities of Si clusters in the size range $1 \leqslant N \leqslant 20$. The calculations confirm and extend earlier theoretical results [7] that show static polarizabilities for Si clusters are larger than the bulk limit based on the Clausius-Mossotti relation. We find no connection between the values of α and either the HOMO-LUMO gap or the cluster dipole moment. Instead the polarizability appears most closely related to the overall shape of the clusters. The polarizability of prolate clusters is about 10% larger than that of compact clusters at the same cluster size. This suggests that measurements of the polarizability could be useful as a probe of cluster shape, complementing the results of ion mobility experiments [19]. Because the cluster polarizability is less sensitive to local atomic rearrangements than other properties like the gap and dipole moment, it is arguably the best indicator of the development of bulklike electronic behavior in clusters. It therefore will be interesting to extend these calculations to larger cluster sizes as more structures become available.

ACKNOWLEDGMENTS

The authors would like to thank Professor Martin Jarrold and Alexander Shvartsburg for valuable discussions. K.A.J. was supported in part by a grant from the National Science Foundation, (Grant No. RUI-DMR940985), and by a grant from the Faculty Research and Creative Endeavors Committee at Central Michigan University. MRP was supported in part by the ONR Georgia Tech Molecular Design Institute (Grant No. N00014-97-1-116). Ames Laboratory is operated for the U.S. Department of Energy by Iowa State University under Contract No. W-7405-Eng-82. K.M.H. and C.Z.W. acknowledge the support of the Director of Energy Research, Office of Basic Energy Sciences, U.S. Department of Energy.

[1] K. M. Ho, A. A. Shvartsburg, B. Pan, Z.-Y. Lu, C.-Z Wang, J. G. Wacker, J. L. Fye, and M. F. Jarrold, Nature (London) **392**, 582 (1998).
[2] P. Hohenberg and W. Kohn, Phys. Rev. **136**, B864 (1964).
[3] W. Kohn and L. J. Sham, Phys. Rev. **140**, A1133 (1965).
[4] B. Liu, A. A. Shvartsburg, Z.-Y. Lu, B. Pan, C.-Z. Wang, K.-M. Ho, and M. F. Jarrold, J. Chem. Phys. **109**, 9401 (1998).
[5] A. A. Shvartsburg, M. F. Jarrold, B. Liu, Z.-Y. Lu, C.-Z. Wang, and K.-M. Ho, Phys. Rev. Lett. **81**, 4616 (1998).
[6] R. Schäfer, S. Schlecht, J. Woenckhaus, and J. A. Becker, Phys. Rev. Lett. **76**, 471 (1996).
[7] I. Vasiliev, S. Ogut, and J. R. Chelikowsky, Phys. Rev. Lett. **78**, 4805 (1997).
[8] A. Sieck D. Porezag, Th. Frauenhein, M. R. Pederson, and K. Jackson, Phys. Rev. A **56**, 4890 (1997).
[9] A. Rubio, J. A. Alonso, X. Blase, L. C. Balbas, and S. G. Louie, Phys. Rev. Lett. **77**, 247 (1996); **77**, 5442 (1996).
[10] K. A. Jackson, M. R. Pederson, D. V. Porezag, Z. Hajnal, and Th. Frauenheim, Phys. Rev. B **55**, 2549 (1997).
[11] D. V. Porezag and M. R. Pederson, Phys. Rev. B **54**, 7830 (1996).
[12] We find it convenient to work in atomic units to compute energies, etc. Relevant conversions are 1 V/m$=5.15 \times 10^{11}$ a.u. for electric fields and 2.5418 D = 1 a.u. for dipole moments. For polarizabilities, 1 Å$^3=(0.529$ a.u.$)^3$ and, of course, 27.2 eV = 1 a.u. is the Hartree atomic unit of energy.
[13] M. R. Pederson and K. A. Jackson, Phys. Rev. B **41**, 7453 (1990).
[14] K. A. Jackson and M. R. Pederson, Phys. Rev. B **42**, 3276 (1990).
[15] M. R. Pederson, K. Jackson, D. V. Porezag, Z. Hajnal, and Th. Frauenheim, Phys. Rev. B **54**, 2863 (1996).
[16] J. P. Perdew, K. Burke, and M. Ernzerhof, Phys. Rev. Lett. **77**, 3865 (1996).
[17] J. Guan, M. E. Casida, A. M. Köster, and D. R. Salahub, Phys. Rev. B **52**, 2184 (1995).
[18] Y.-M. Juan, E. Kaxiras, and R. G. Gordon, Phys. Rev. B **51**, 9521 (1995).
[19] M. F. Jarrold and V. A. Constant, Phys. Rev. Lett. **67**, 2994 (1992).
[20] R. Schäfer, J. Woenckhaus, J. A. Becker, and F. Hensel, Z. Naturforsch. A **50a**, 445 (1995).
[21] J. A. Becker, Angew. Chem. Int. Ed. Engl. **36**, 1390 (1997).
[22] W. A. de Heer, Rev. Mod. Phys. **65**, 611 (1993).
[23] E. Benichou, R. Antoine, D. Rayane, B. Vezin, F. W. Dalby, Ph. Dugourd, M. Broyer, C. Ristori, F. Chandezon, B. A. Huber, J. C. Rocco, S. A. Blundell, and C. Guet, Phys. Rev. A **59**, R1 (1999).
[24] J. P. Perdew, J. A. Chevary, S. H. Vosko, K. A. Jackson, M. R. Pederson, D. J. Singh, and C. Fiolhais, Phys. Rev. B **46**, 6671 (1992).
[25] K. A. Jackson (unpublished).